Arch. Mech., 38, 4, pp. 473–491, Warszawa 1986

Viscoelastic flow between two rotating cylinders: application to rolling or calendering processes

S. ZAHORSKI (WARSZAWA)

THE PREVIOUSLY developed concept of plane flows with dominating extensions [11] is applied to the nip region of viscoelastic flow between two rotating cylinders. Some approximate solutions are derived for incompressible viscoelastic fluids with an arbitrary extensional viscosity function. Under the assumption of small variability of this function, possible distributions of thrusts, total loads, friction forces and coefficients, etc, are discussed in greater detail. Some comparisons with experimental data are also presented.

Poprzednio rozwiniętą koncepcję płaskich przepływów z dominującym rozciąganiem [11] zastosowano do przepływu lepkosprężystego w obszarze bezpośrednio między dwoma obracającymi się walcami. Pewne przybliżone rozwiązania wyprowadzono dla nieściśliwych cieczy lepkosprężystych z dowolnymi funkcjami lepkości przy rozciąganiu. W założeniu małej zmienności tych funkcji, przedyskutowano bardziej szczegółowo możliwe rozkłady nacisków, całkowitych obciążeń, sił tarcia i współczynników tarcia, itp. Przedstawiono również pewne porównania z danymi doświadczalnymi.

Раньше развернутая концепция плоских течений с доминирующим растяжением [11] применена к вязкоупругому течению в области непосредственно между двумя вращающимися цилиндрами. Некоторые приближенные решения выведены для несжимаемых вязкоупругих жидкостей с произвольными функциями вязкости при растяжении. В предположении малой переменности этих функций обсуждены более подробно возможные распределения нажимов, полных нагружений, сил трения и коэффициентов трения и т. п. Представлено тоже некоторое сравнение с экспериментальными данными.

1. Introduction

STARTING from the early contributions of G. B. Jeffrey, Th. von Kármán, G. I. Taylor and others, the problem stated under the title has been extensively studied, mainly for Newtonian and simple inelastic fluids (cf. [1, 2, 3, 4]). Only very few analytical solutions have been obtained for viscoelastic or elastic models and compared with available experimental data (cf. [5, 6, 7, 8, 9]). The importance of flows between rotating cylinders considered with appropriate kinematic and dynamic boundary conditions results from many practical applications to various lubricating systems as well as to milling, rolling, calendering and even printing processes. Although at present there is no doubt about the role played by essentially very large extensional gradients in the geometry considered, there still exist some controversies concerned with the possible effects of viscoelastic properties (cf. [5, 9, 10]).

In the present paper the problem of viscoelastic flow between two rotating cylinders is treated as a thin-layer „flow with dominating extensions" (FDE), the concept of which,

developed in our previous paper [11], was inspired by A. B. METZNER's idea of extensional primary field approximations [12,5]. To this end, we briefly discuss the corresponding governing equations for plane steady flows with dominating extensions. As a next step, some approximate solutions valid in the nip region between two rotating cylinders are presented for viscous Newtonian as well as for incompressible viscoelastic fluids with an arbitrary dependence of the extensional viscosity function on the extension rate. More detailed results are also derived for relatively small variability of the extensional viscosity function. The resulting distributions of thrusts, total loads, friction forces and coefficients are considered in greater detail and the effects of various forms of the extensional viscosity functions discussed. Few words are also devoted to flows in the so-called rolling bank region, and to possible effects of viscoelastic properties.

2. Governing equations for plane flows with dominating extensions (FDE)

Consider plane steady flows, the Cartesian velocity components of which can be presented in the following form (cf. [11]):

$$\begin{aligned} u^* &= qx+u(x,y), \\ v^* &= -qy+v(x,y), \end{aligned} \tag{2.1}$$

where $q = U/h_0$ is some constant extension gradient, and u and v denote additional velocity components directed along the axes x and y, respectively. If, moreover, one of the characteristic dimensions L (in the x-direction) is much greater than the other h_0 (in the y-direction, respectively), we can use all simplifications resulting from the so-called lubrication approximation for small $\varepsilon = h_0/L \ll 1$.

Under the above assumptions, the velocity gradient and vorticity components can be expressed as

$$\begin{aligned} &\frac{\partial u^*}{\partial x} = q\left(1+\varepsilon\frac{\partial \bar{u}}{\partial \bar{x}}\right), \quad \frac{\partial u^*}{\partial y} = q\frac{\partial \bar{u}}{\partial \bar{y}}, \\ &\frac{\partial v^*}{\partial x} = q\varepsilon^2\frac{\partial \bar{v}}{\partial \bar{x}}, \quad \frac{\partial v^*}{\partial y} = q\left(-1+\varepsilon\frac{\partial \bar{v}}{\partial \bar{y}}\right), \\ &\omega^* = \frac{1}{2}q\left(\frac{\partial \bar{u}}{\partial \bar{y}} - \varepsilon^2\frac{\partial \bar{v}}{\partial \bar{x}}\right), \end{aligned} \tag{2.2}$$

where U denotes a characteristic velocity and the overbars refer to the dimensionless quantities introduced as follows:

$$x = L\bar{x}, \quad y = h_0\bar{y}, \quad u = U\bar{u}, \quad v = \varepsilon U\bar{v}, \quad q = \frac{U}{L_0}\bar{q}. \tag{2.3}$$

For flows with relatively small vorticity components (or relatively high Deborah numbers, [11, 12]), it may happen that the first terms in the diagonal components described by Eq. (2.2) are essentially greater than the remaining terms. To this end, it is sufficient to assume that the dimensionless components of additional velocity gradients are, at the most, of order $O(1)$.

In our paper [11] we defined the plane "flows with dominating extensions" (FDE) as such thin-layer flows for which the constitutive equations, exact for purely extensional flows of an incompressible simple fluid (cf. [11, 14]), can be used in a linear form perturbed with respect to the extension rate q. This assumption leads to the following constitutive equations:

$$\mathbf{T}^* = -p\mathbf{1}+\mathbf{T}_E^* = -p\mathbf{1}+\beta(q)\mathbf{A}_1+\beta(q)\mathbf{A}_1'+\frac{d\beta}{dq}\mathbf{A}_1 q', \tag{2.4}$$

where p is a scalar pressure term, $\mathbf{A}_1$ denotes the first Rivlin–Ericksen kinematic tensor (cf. [14]), and the primes denote the corresponding linear increments, i.e. $\mathbf{A}_1' = \mathbf{A}_1^*-\mathbf{A}_1$, $q' = q^*-q'$, etc., resulting from Eqs. (2.1).

It is noteworthy that the material function $\beta(q)$, hereafter called the extensional viscosity function, is simply related to the planar extensional (elongational) viscosity, viz.

$$\eta^*(q) = \frac{1}{q}(T^{*11}-T^{*22}) = 4\beta(q). \tag{2.5}$$

After introducing Eqs. (2.1) and (2.4) into the corresponding equations of equilibrium with inertia terms disregarded([1]), we obtain the set of two equations involving terms of different orders of magnitude with respect to small parameter $\varepsilon = h_0/L$. Expressing these equations in a dimensionless form, by means of Eqs. (2.3) and

$$p = \frac{U\eta L}{h_0^2}\bar{p}, \quad \beta(q) = \eta\bar{\beta}(q), \tag{2.6}$$

where η is a viscosity constant, and retaining only terms of the highest order of magnitude with respect to ε, i.e. the terms of order $O(1)$, we arrive at the following equations (in dimensional forms):

$$\frac{dp^*}{dx} = \frac{1}{2}\frac{d\beta}{dq}\frac{\partial}{\partial x}\left(\frac{\partial u}{\partial y}\right)^2+\beta\frac{\partial^2 u}{\partial y^2}, \quad \frac{\partial p^*}{\partial y} = 0, \tag{2.7}$$

where

$$p^* = p-T_E^{*22} = p+2\beta q+\frac{1}{4}\frac{d\beta}{dq}\left(\frac{\partial u}{\partial y}\right)^2 \tag{2.8}$$

denotes a modified pressure (thrust). Eliminating the pressure terms from Eqs. (2.7), we have alternatively

$$\frac{\partial}{\partial y}\left[\frac{1}{2}\frac{d\beta}{dq}\frac{\partial}{\partial x}\left(\frac{\partial u}{\partial y}\right)^2+\beta\frac{\partial^2 u}{\partial y^2}\right] = 0. \tag{2.9}$$

It is also noteworthy that the following simplified constitutive equations:

$$T^{*11} = -p+2\beta q+\frac{1}{4}\frac{d\beta}{dq}\left(\frac{\partial u}{\partial y}\right)^2, \tag{2.10}$$

([1]) The inertia effects can be taken into account in an approximate way by means of the total balance of mass (cf. [11, 13]).

(2.10) [cont.]
$$T^{*22} = -p - 2\beta q - \frac{1}{4}\frac{d\beta}{dq}\left(\frac{\partial u}{\partial y}\right)^2,$$
$$T^{*12} = \beta\frac{\partial u}{\partial y}$$

directly lead to Eqs. (2.7) or (2.9).

Equation (2.9) is a third-order nonlinear partial differential equation, the solution of which, even for entirely specified boundary conditions, is not known. In the paper [11] we looked for an approximate solution in a form linearly depending on the x coordinate, viz.

(2.11) $$u = (x+a)\,(w(y)+b),$$

where a and b are constants and w denotes a function of y only. Introducing Eq. (2.11) into Eq. (2.9), we arrive at

(2.12) $$(x+a)\left(\beta w''(y) + \frac{d\beta}{dq}\,w'^2(y)\right) = \frac{dp^*}{dx},$$

where the primes denote derivatives with respect to y. It can easily be observed that any solution w of the simplified equation

(2.13) $$\beta w''(y) + \frac{d\beta}{dq}\,w'^2(y) = C = \text{const}$$

also satisfies Eq. (2.12) if $dp^*/dx = C(x+a)$, i.e. for a parabolic dependence of p^* on x. Other distributions of thrusts can be described reasonably, assuming that $C = C(x)$, where x is treated as a parameter involved in the solution of Eq. (2.13).

Equation (2.13) is a special Riccati equation for $w'(y)$, and its general solution symmetrical with respect to y ($w'(0) = 0$) can be presented as

(2.14)
$$w(y) = \frac{1}{A}\ln\cos\sqrt{-ABy^2} + C_1 \quad \text{for} \quad AB < 0,$$
$$w(y) = \frac{1}{A}\ln\operatorname{ch}\sqrt{ABy^2} + C_1 \quad \text{for} \quad AB > 0,$$

where C_1 is an integration constant and

(2.15) $$A = \frac{1}{\beta}\frac{d\beta}{dq}, \qquad B = \frac{C}{\beta} = \frac{1}{(x+a)\beta}\frac{dp^*}{dx}.$$

The values of $A > 0$ correspond to increasing extensional viscosity functions $\beta(q)$, while those of $A < 0$ — to decreasing $\beta(q)$. The sign of the product AB depends, therefore, on the sign of C, i.e. on whether the thrust p^* is an increasing or decreasing function of x.

3. Solutions in the nip region between two rotating cylinders

In the present section the solutions derived for plane FDE are used in the case of flow between two rotating cylinders, i.e. in the situation typical for rolling or calendering

processes (Fig. 1). We assume, moreover, that the rollers of the same radii R rotate with constant tangential velocity V, and the smallest distance between them at the nip cross-section is $2h_0$.

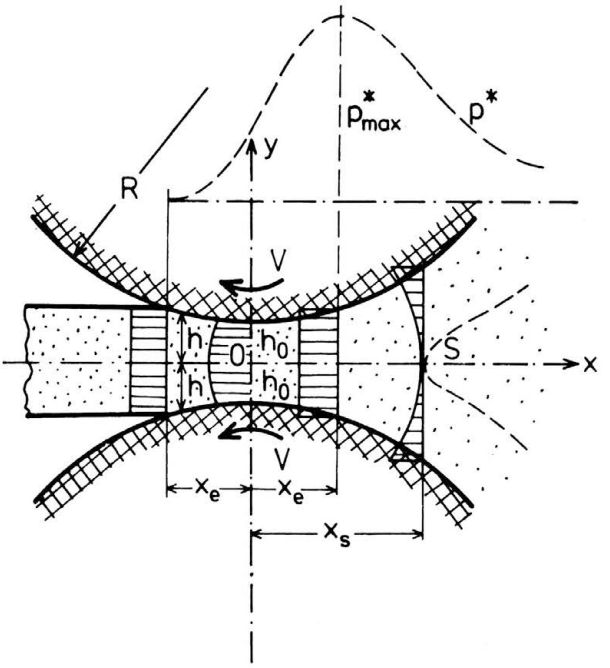

FIG. 1.

Being interested in approximate solutions valid only in the nip region, we assume as usuall that (cf. [2, 4])

$$L = \sqrt{2h_0 R}, \qquad \varepsilon = h_0/L, \qquad h = h_0\left(1+\frac{x^2}{L^2}\right), \tag{3.1}$$

where the last relation introduces a parabolic dependence of the distance between cylinder surfaces h on x, valid for small ratios x/L.

The problem considered can be solved for various modified boundary conditions, especially those prescribed at the entry or exit cross-sections (cf. [1, 2, 3, 4]).

3.1. Boundary conditions

When a fluid fully adheres to the surfaces of rollers, it is usually assumed that (cf. [1, 2, 4])

$$u^* = -V \quad \text{for} \quad y = \pm h, \tag{3.2}$$

where the minus sign indicates that the cylinders rotate from right to left as in Fig. 1. At the exit cross-section, where the fluid leaves the rollers, a uniform velocity distribution with respect to y requires that

$$u^* = -V = \text{const} \quad \text{for} \quad x = -x_e; \tag{3.3}$$

what is equivalent (cf. Eq. $(2.10)_3$) to

$$T^{*12} = 0 \quad \text{for} \quad x = -x_e. \tag{3.4}$$

We assume, moreover, that the modified pressure (thrust) distributions satisfy the Reynolds-type boundary conditions (cf. [2, 4]), viz.

$$\begin{aligned} &p^* = 0 \text{ (or const)}, \quad \frac{dp^*}{dx} = 0 \quad \text{for} \quad x = -x_e, \\ &p^* = 0 \text{ (or const)} \quad \text{for} \quad x \to \infty. \end{aligned} \tag{3.5}$$

Other kinds of boundary conditions, e.g. those describing the existence of a cavitation pocket at the exit area (cf. [9, 15]), can also be taken into account.

A position x_s of the stagnation point indicating presence of the reversed flow region results from the requirement

$$u^* = 0 \quad \text{for} \quad x = x_s, \quad y = 0. \tag{3.6}$$

In what follows, we shall use the following dimensionless coordinates:

$$\xi = \frac{x}{L}, \quad \lambda = \frac{x_e}{L}, \quad \xi_s = \frac{x_s}{L}; \tag{3.7}$$

thus

$$h = h_0(1+\xi^2), \quad h_e = h_0(1+\lambda^2), \quad h_s = h_0(1+\xi_s^2). \tag{3.8}$$

According to Eqs. $(2.1)_1$ and (2.14), the x-component of the velocity field can be written as

$$u^* = -qx + \frac{1}{A}(x-x_e)\left(\ln\cos\sqrt{-ABy^2} + C_1\right), \tag{3.9}$$

and, after introducing $q = V/x_e$ and taking into account Eq. (3.2), as

$$u^* = -V + \frac{1}{A}(x-x_e)\left(\ln\cos\sqrt{-ABy^2} - \ln\cos\sqrt{-ABh^2}\right) \tag{3.10}$$

for $AB < 0$. If $AB > 0$, the cosine terms must be replaced by their hyperbolic counterparts.

By way of illustration of the method used in this paper, we begin with the case of purely viscous Newtonian fluids for which the corresponding solutions have been obtained elsewhere (cf. [1, 2, 3, 4]).

3.2. Newtonian case

In the Newtonian case ($\beta = \beta_0 = \text{const}$, $d\beta/dq = 0$) a solution can be obtained either directly from the simplified Eq. (2.13) or by expanding the logarithmic terms in Eq. (3.10) into series for small values of A and retaining first linear terms. Both procedures lead to the same result:

$$u_N^* = -V + (x-x_e)\frac{C_N}{2\beta_0}(y^2-h^2) = -V + \frac{1}{2\beta_0}\left(\frac{dp^*}{dx}\right)_N (y^2-h^2), \tag{3.11}$$

where the subscript N indicates Newtonian quantities.

Assuming that the volumetric rate Q per unit length of a cylinder (volume discharge) is conserved during steady-state flow, viz.

$$Q = 2Vh_e = -2\int_0^h u^* dy = \text{const}, \tag{3.12}$$

we have either

$$C_N = -\frac{3\beta_0 V}{x-x_e}\frac{h-h_e}{h^3} = -\frac{3\beta_0 V}{Lh_0^2}\frac{\xi+\lambda}{(1+\xi^2)^3}, \tag{3.13}$$

or

$$\left(\frac{dp^*}{dx}\right)_N = (x-x_e)C_N = -\frac{3\beta_0 V}{h_0^2}\frac{\xi^2-\lambda^2}{(1+\xi^2)^3}, \tag{3.14}$$

where Eqs. (3.7) and (3.8) have been taken into account. Substituting Eq. (3.13) into Eq. (3.11), we arrive at the well-known velocity distribution

$$u_N^* = -V\left[1-\frac{3}{2}\frac{\xi^2-\lambda^2}{1+\xi^2}\left(1-\frac{y^2}{h^2}\right)\right] \tag{3.15}$$

satisfying the kinematic boundary conditions (3.2) and (3.3).

For the Newtonian volumetric rate, we obtain from Eq. (3.12)

$$Q_N = 2Vh_0(1+\lambda^2). \tag{3.16}$$

The stagnation point dimensionless coordinate ξ_{sN} results directly from Eq. (3.15) if the condition (3.6) is used. Thus we arrive at

$$\xi_{sN}^2 = 2+3\lambda^2 \qquad (h_s = 3h_e). \tag{3.17}$$

In agreement with the boundary conditions valid for modified pressures (3.5), we can write

$$p_{\text{exit}}^* - p_\infty^* = \int_{-x_e}^{\infty} \frac{dp^*}{dx}\,dx = 0. \tag{3.18}$$

Integration of the expression described by Eq. (3.14) leads to the following transcendental equation for the dimensionless quantity λ:

$$\lambda(1+3\lambda^2)+(3\lambda^2-1)\left(\operatorname{arctg}\lambda+\frac{\pi}{2}\right)(1+\lambda^2) = 0, \tag{3.19}$$

the numerical solution of which gives $\lambda = 0.6798$[2].

The thrust distribution in the Newtonian case can be presented as

$$p_N^* = \frac{3\beta_0 V}{4h_0}\sqrt{\frac{R}{2h_0}}\left[\frac{2\xi}{(1+\xi^2)^2}(1+\lambda^2)+(3\lambda^2-1)\left(\frac{\xi}{1+\xi^2}+\operatorname{arctg}\xi\right)+C_2\right], \tag{3.20}$$

[2] It is amazing that for exactly the same form of Eq. (3.19), J. R. A. PEARSON [4], obtained $\lambda = 0.475$ (!); thus other numerical results are entirely different.

where C_2 is a new integration constant. If we assume, moreover, that $p^*(-\lambda) = p^*(\infty) = 0$, we arrive at

$$C_2 = \frac{\lambda(1+3\lambda^2)}{1+\lambda^2} + (3\lambda^2-1)\operatorname{arctg}\lambda = -\frac{\pi}{2}(3\lambda^2-1). \tag{3.21}$$

Hence the maximum thrust (for $\xi = \lambda$) is expressed as

$$(p^*_{\max})_N = \frac{3\beta_0 V}{4h_0}\sqrt{\frac{R}{2h_0}}\left[\frac{\lambda(1+3\lambda^2)}{1+\lambda^2} - (3\lambda^2-1)\left(\frac{\pi}{2} - \operatorname{arctg}\lambda\right)\right] = \frac{3\beta_0 V}{4h_0}\sqrt{\frac{R}{2h_0}}\,\pi(1-3\lambda^2). \tag{3.22}$$

It is noteworthy that the value of thrust at the nip cross-section, i.e. for $x = \xi = 0$, is equal to half of the maximum value, viz. $p^*(0)_N = \frac{1}{2}(p^*_{\max})_N$.

We can easily verify that the results obtained so far for the Newtonian case are, apart from certain numerical differences, in satisfactory agreement with those known from references (cf. [2, 4]).

3.3. General viscoelastic case

In the case of general viscoelastic fluid ($\beta = \beta(q)$, $d\beta/dq \neq 0$), we introduce the following new quantities:

$$K = \frac{AV}{L} = \frac{V}{\beta L}\frac{d\beta}{dq}, \qquad \gamma = AHq = KH\frac{\xi+\lambda}{1+\xi^2}, \tag{3.23}$$

where H, by analogy to Eq. (3.13), is defined as the corresponding coefficient in the relationship

$$C = -H\frac{\beta(q)V}{x-x_e}\frac{h-h_e}{h^3} = -H\frac{\beta(q)V}{Lh_0^2}\frac{\xi+\lambda}{(1+\xi^2)^3}; \tag{3.24}$$

H itself may depend on ξ or γ, and for the Newtonian case ($\beta = \beta_0$), we have $H = 3$.

Bearing in mind that according to our new notations

$$-ABy^2 = \frac{1}{\beta}\frac{d\beta}{dq}\frac{C}{\beta}y^2 = KH\frac{\xi+\lambda}{1+\xi^2}\frac{y^2}{h^2} = \gamma\frac{y^2}{h^2}, \tag{3.25}$$

Eq. (3.10) leads to the following velocity distribution:

$$u^* = -V\left[1 - \frac{\xi-\lambda}{K}\left(\ln\cos\sqrt{\gamma\frac{y^2}{h^2}} - \ln\cos\sqrt{\gamma}\right)\right], \tag{3.26}$$

for $\gamma > 0$ ($K > 0$), and to a similar expression with cosine terms replaced by hyperbolic cosine terms, for $\gamma < 0$ ($K < 0$).

Performing integration shown in Eq. (3.12), we also arrive at the conditions

$$\frac{\gamma}{H} = -\left[\ln\cos\sqrt{\gamma} + \frac{1}{\sqrt{\gamma}}\mathrm{L}(\sqrt{\gamma})\right] \quad \text{for} \quad \gamma > 0, \tag{3.27}$$

$$\frac{\gamma}{H} = \left[\ln\operatorname{ch}\sqrt{-\gamma} - \frac{1}{\sqrt{-\gamma}}\bar{\mathrm{L}}(\sqrt{-\gamma})\right] \quad \text{for} \quad \gamma < 0, \tag{3.28}$$

where

$$\text{(3.29)} \qquad \mathrm{L}(x) = -\int_0^x \ln\cos z\,dz, \quad \bar{\mathrm{L}}(x) = \int_0^x \ln\mathrm{ch}\, z\,dz$$

denote the ordinary and modified Lobachevsky functions (cf. [16]), respectively, the diagrams of which have been presented in the paper [11]. Equations (3.27) and (3.28) express implicit relations between the quantities H and γ; they also depend on the viscoelasticity coefficient K defined in Eq. $(3.23)_1$, the parameter λ and the distance ξ.

It can easily be observed that $\gamma = 0$ either for $K = 0$ (the Newtonian case) or for $\xi = -\lambda$ (at the exit); otherwise the values of γ essentially depend on $K \neq 0$. The exact dependence of H on positive and negative γ is shown with bold solid lines in Fig. 2.

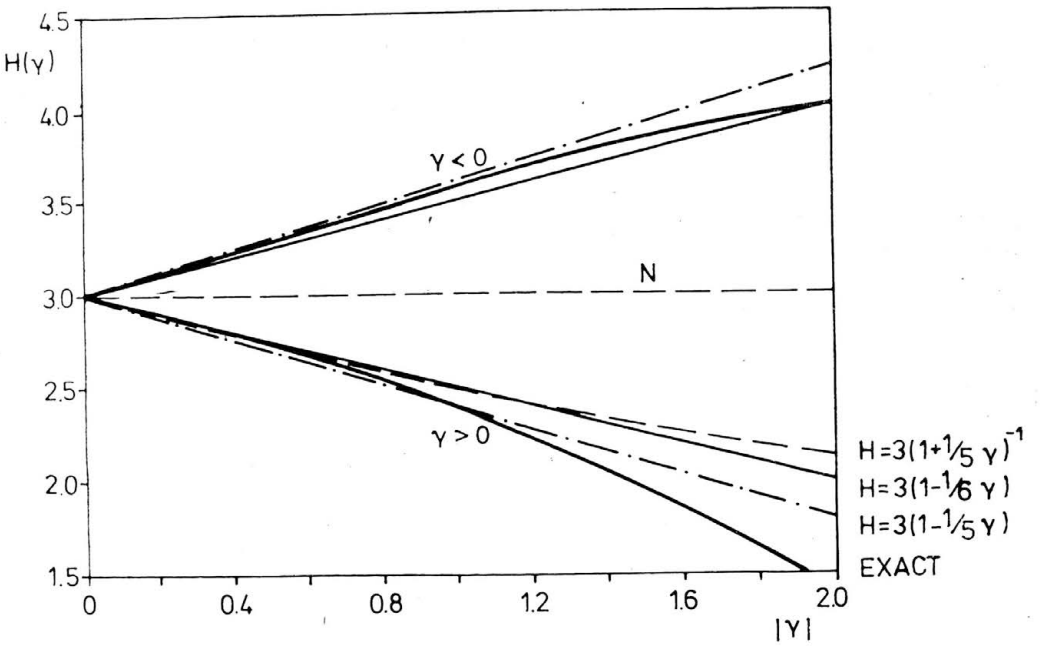

FIG. 2.

In a similar way, it can be proved that the volumetric rate per unit length of a cylinder can be expr essed as

$$\text{(3.30)} \qquad Q = 2Vh_0\left\{1-\frac{\lambda}{K}\left[\ln\cos\sqrt{\gamma}+\frac{1}{\sqrt{\gamma}}\mathrm{L}(\sqrt{\gamma})\right]\right\} \qquad \text{for} \quad \gamma > 0,$$

$$\text{(3.31)} \qquad Q = 2Vh_0\left\{1-\frac{\lambda}{K}\left[\ln\mathrm{ch}\sqrt{-\gamma}-\frac{1}{\sqrt{-\gamma}}\bar{\mathrm{L}}(\sqrt{-\gamma})\right]\right\} \qquad \text{for} \quad \gamma < 0.$$

The stagnation point coordinate ξ_s results from the equation

$$\text{(3.32)} \qquad \cos\sqrt{\gamma} = \exp\left(-\frac{K}{\xi_s-\lambda}\right),$$

where, for $\gamma < 0$ ($K < 0$), the term $\cos\sqrt{\gamma}$ must be replaced by $\mathrm{ch}\sqrt{-\gamma}$.

An equivalent of Eq. (3.19), leading to the functional dependence $\lambda(K)$, can be achieved from

$$\int_{-\lambda}^{\infty} H \frac{\beta(q) VL}{h_0^2} \frac{\xi^2-\lambda^2}{(1+\xi^2)^3}\, d\xi = 0, \tag{3.33}$$

bearing in mind that H depends on ξ through γ defined in Eq. $(3.23)_2$.

Almost all the formulae discussed in the present subsection are too complex for direct and successful numerical computations. For the sake of simplicity, we shall apply some expansions, using the fact that the viscoelasticity coefficient K, defined by Eq. $(3.23)_1$, may be very small even for very high velocities V. Such an assumption seems to be valid for fluids for which, even at large values of the extensional viscosity $\beta(q)$, its variability with increasing velocities of extension rates is rather weak.

3.4. Viscoelastic case for a weak variability of the extensional viscosity function

Under the assumption of small K, it is seen from Eq. (3.23) that γ is a small quantity, especially in the vicinity of the exit ($\xi = -\lambda$) or the nip ($\xi = 0$) cross-sections. Thus all the relations obtained for the general case can be presented in more explicit forms by expanding them into a series in the neighbourhood of $K = 0$.

Therefore, retaining only terms linear with respect to K, we have from Eq. (3.26)

$$u^* = -V\left\{1-\frac{H}{2}\frac{\xi^2-\lambda^2}{1+\xi^2}\left[\left(1-\frac{y^2}{h^2}\right)+\frac{KH}{6}\frac{\xi+\lambda}{1+\xi^2}\left(1-\frac{y^4}{h^4}\right)\right]\right\} \tag{3.34}$$

for $K > 0$ as well as for $K < 0$. Exactly at the nip cross-section ($\xi = 0$), we obtain

$$u^*|_0 = -V\left\{1+\frac{H}{2}\lambda^2\left[\left(1-\frac{y^2}{h^2}\right)+\frac{KH}{6}\lambda\left(1-\frac{y^4}{h^4}\right)\right]\right\}, \tag{3.35}$$

and

$$\left.\frac{\partial u^*}{\partial y}\right|_0 = \frac{VH\lambda^2}{h^2} y\left(1+\frac{1}{3}KH\lambda\frac{y^2}{h^2}\right). \tag{3.36}$$

Thus the shape of the velocity profile essentially depends on K and H. To decide whether it is more prolate or oblate as compared with the Newtonian case, one should know the functional dependence $\lambda(K)$.

It is seen that either integration of Eq. (3.34) or expansion of Eqs. (3.27) and (3.28) and retaining terms linear with respect to K, lead to

$$1 = \frac{H}{3}\left(1+\frac{1}{5}KH\frac{\xi+\lambda}{1+\xi^2}\right) = \frac{H}{3}\left(1+\frac{1}{5}\gamma\right). \tag{3.37}$$

Instead of seeking formal solutions of Eq. (3.37), we shall use the following linear expressions:

$$\text{(I)}\quad H = 3\left(1-\frac{1}{5}\gamma\right), \qquad \text{(II)}\quad H = 3\left(1-\frac{1}{6}\gamma\right) \tag{3.38}$$

shown in Fig. 2 for $\gamma > 0$ as well as for $\gamma < 0$. The broken line (I) gives better fit to the

exact solution for greater values of γ, while the solid line (II) can be used alternatively for small γ.

For practical purposes, it is much more useful to introduce a direct dependence of H on K. Assuming that for $\gamma = 1$, $H = 2.4$ and $H = 2.5$, respectively for the case (I) and (II), we have

$$(3.39) \qquad \text{(I)} \quad H = 3\left(1 - \frac{12}{25} K \frac{\xi+\lambda}{1+\xi^2}\right), \qquad \text{(II)} \quad H = 3\left(1 - \frac{5}{12} K \frac{\xi+\lambda}{1+\xi^2}\right),$$

if $K > 0$, and similar expressions with the ratios 18/25 and 6/12 in the parentheses if $K < 0$. It must be emphasized that Eqs. (3.39) ensure even more accurate results than the linear approximations described by Eqs. (3.38).

Introducing Eqs. (3.39) into Eq. (3.34), and disregarding terms of order ε^2, we arrive at

$$(3.40) \qquad u^* = -V\left\{1 - \frac{3}{2}\frac{\xi^2-\lambda^2}{1+\xi^2}\left[\left(1-\frac{y^2}{h^2}\right) - \frac{12}{25} K \frac{\xi+\lambda}{1+\xi^2}\left(1-\frac{y^2}{h^2}\right) + \frac{1}{2} K \frac{\xi+\lambda}{1+\xi^2}\left(1-\frac{y^4}{h^4}\right)\right]\right\}$$

for the case (I), and a similar expression with 5/12 instead of 12/25 for the case (II).

The volumetric rate per unit length of cylinder amounts to

$$(3.41) \qquad Q = 2Vh_0\left(1+\lambda^2+\frac{3}{25}K\lambda^3\right),$$

where the ratio 3/25 should be replaced by 11/60 for the case (II).

The stagnation point coordinate results from the equation

$$(3.42) \qquad 1 = \frac{\xi_s^2-\lambda^2}{1+\xi_s^2}\frac{H}{2}\left(1+\frac{1}{6}KH\frac{\xi_s+\lambda}{1+\xi^2}\right),$$

which, after substituting for H from the approximations (3.39), leads to

$$(3.43) \qquad \text{(I)} \quad \xi_s^2 = 2+3\lambda^2-\frac{k}{5}(\xi_{sN}+\lambda), \qquad \text{(II)} \quad \xi_s^2 = 2+3\lambda^2-\frac{5}{6}k(\xi_{sN}+\lambda),$$

if $k = 1/5\ K > 0$. In the above derivation we used the Newtonian value ξ_{sN} defined in Eq. (3.17) and retained terms linear with respect to $k = K/5$.

The equivalent of Eq. (3.14), viz.

$$(3.44) \qquad \frac{dp^*}{dx} = (x-x_e)C = -H\frac{\beta(q)VL}{h_0^2}\frac{\xi^2-\lambda^2}{(1+\xi^2)^3},$$

after using Eqs. (3.39) and integrating, gives

$$(3.45) \qquad p^* = \frac{\beta_0}{\beta}p_N^* + \frac{3\beta V}{4h_0}\sqrt{\frac{R}{2h_0}}\left(\frac{4}{5}k\right)\left[(1-5\lambda^2)\left(\frac{\lambda\xi}{(1+\xi^2)^2}+\frac{3}{2}\frac{\lambda\xi}{1+\xi^2} + \frac{3}{2}\lambda\operatorname{arctg}\xi\right) - \frac{1}{(1+\xi^2)^3}(4\lambda\xi+4\lambda^3\xi+6\xi^2-4\lambda^2+2) + C_2\right],$$

where the ratio 4/5 should be replaced by 25/36 for the case (II).

The dependence of λ on k (or K) can be calculated on the basis of Eq. (3.33). This leads to the following transcendental equation:

$$(3.46)\quad (1+\lambda^2)^2\left[\lambda(1+3\lambda^2)+(3\lambda^2-1)\left(\frac{\pi}{2}+\operatorname{arctg}\lambda\right)(1+\lambda^2)\right]$$
$$=\frac{4}{5}k\left\{4\lambda^4+2\lambda^2-2+(5\lambda^2-1)\left[\lambda^2(1+\lambda^2)\right.\right.$$
$$\left.\left.+\frac{3}{2}\lambda^2(1+\lambda^2)^2+\frac{3}{2}\lambda(1+\lambda^2)^3\left(\frac{\pi}{2}+\operatorname{arctg}\lambda\right)\right]\right\},$$

where again the ratio 25/36 replaces 4/5 in the case (II). The above equation has two groups of roots for k varying between 0 and 1. Being exclusively interested in solutions valid for sufficiently small positive k, we do not intend to decide at the moment, whether the existence of the other group of roots (for $k > 0.6$) is an artefact or may have any physical meaning. Some illustrative values of roots of the first group are shown in Table 1.

Table 1. Numerical values of λ as function of k.

k														
	(I)	0	0.063	0.125	0.188	0.250	0.313	0.375	0.438	0.500	0.563	0.625	0.688	0.750
	(II)	0	0.072	0.144	0.216	0.288	0.360	0.432	0.504	0.576	0.648	0.720	0.792	0.854
$\lambda(k)$		0.680	0.673	0.665	0.655	0.643	0.627	0.605	0.574	0.532	0.473	0.398	0.315	0.235

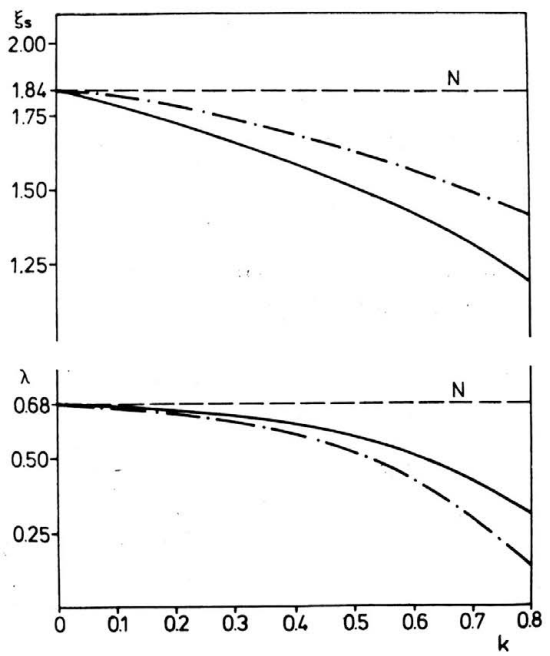

FIG. 3.

The function $\lambda(k)$ for positive k is presented graphically in Fig. 3 where the broken line refers to the case (I), while the solid one — to the case (II). In the same Fig. 3, the function $\xi_s(k)$, i.e. the dimensionless coordinate of the stagnation point is plotted versus $k > 0$, according to Eqs. (3.43). Hence, it is seen that the position of maximum thrust approaches the nip when the viscoelasticity coefficient increases. Similarly the stagnation point for viscoelastic fluids appears closer to the nip as compared with purely viscous Newtonian fluids ($\xi_{sN} = 1.84$). Graphs of the functions $\lambda(k)$ and $\xi_s(k)$ for negative k are anti-symmetric with respect to the axis $k = 0$. Therefore, the effect of negative viscoelasticity coefficients on the behaviour of the maximum thrust position and the stagnation point coordinate is quite opposite to that described previously.

The above statements concerned with the influence of an increasing or decreasing extensional viscosity on the maximum thrust position and the stagnation point coordinate are in agreement, at least qualitatively, with certain experimental observations (cf. [6, 8, 9]).

4. Distributions of maximum thrusts, load and friction forces

4.1. Effect of extensional viscosity

If we assume that $p^*(-\lambda) = p^*(\infty) = 0$, Eq. (3.45) leads to the following expression for the maximum thrust:

$$(4.1)\quad p^*_{\max} = \frac{\beta_0}{\beta}(p^*_{\max})_N + \frac{3\beta V}{4h_0}\sqrt{\frac{R}{2h_0}}\left(\frac{4}{5}k\right)\left[\frac{3}{4}\pi\lambda(5\lambda^2-1)\right.$$
$$\left. -(5\lambda^2-1)\left(\frac{\lambda^2}{(1+\lambda^2)^2}+\frac{3}{2}\frac{\lambda^2}{1+\lambda^2}+\frac{3}{2}\lambda\operatorname{arctg}\lambda\right)-2\frac{2\lambda^4+3\lambda^2+1}{(1+\lambda^2)^3}\right],$$

where the ratio 4/5 should be replaced by 25/36 in the case (II).

Taking into account Eq. (3.22), we can calculate the ratio of $p^*_{\max}$ to $(p^*_{\max})_N$. The resulting quantity has the form of a product of two factors: the ratio of the extensional viscosity to its Newtonian counterpart $\beta(q)/\beta_0$, and the expression depending exclusively on k (λ itself is a function of k). The first factor is proportional to the extensional viscosity function $\beta(q)$, while the second one, depending also on the boundary conditions applied, characterizes variability of the extensional viscosity function with the extension gradient $q = V/L\lambda(k)$. The second factor, i.e. $\beta_0 p^*_{\max}/\beta(p^*_{\max})_N$, is plotted versus k in Fig. 4. This quantity is a monotonically decreasing function, and for various increasing extensional viscosities $\beta(q)$, an overall behaviour of $p^*_{\max}/(p^*_{\max})_N$ may be very different.

Integration of the thrust from the exit ($\xi = -\lambda$) to infinity ($\xi = \infty$), viz.

$$(4.2)\qquad F = \int_{-\lambda}^{\infty} p^*(\xi)\,d\xi,$$

leads to the total load force (load capacity) in the form

$$(4.3)\quad F = \frac{3\beta VR}{4h_0}\left\{1-\lambda(3\lambda^2-1)\left(\operatorname{arctg}\lambda+\frac{\pi}{2}\right)+\left(\frac{4}{5}k\right)\left[\frac{3}{2}(\lambda^2-1)\left(\frac{\lambda}{1+\lambda^2}+\operatorname{arctg}\lambda\right)\right.\right.$$

(4.3) [cont.]
$$-(5\lambda^2-1)\left(\frac{\lambda}{2(1+\lambda^2)}-\frac{3}{2}\lambda^2\operatorname{arctg}\lambda\right)+\frac{3}{4}\pi(5\lambda^4-1)\Bigg]\Bigg\}$$

and a similar expression with 25/36 instead of 4/5 for the case (II). The functional dependence of the ratio $\beta_0 F/\beta F_N$ on $k > 0$ is also shown in Fig. 4. It is noteworthy that for small values of k (up to 0.15), the quantity considered is a little greater than unity, and for higher values of k decreases monotonically below unity.

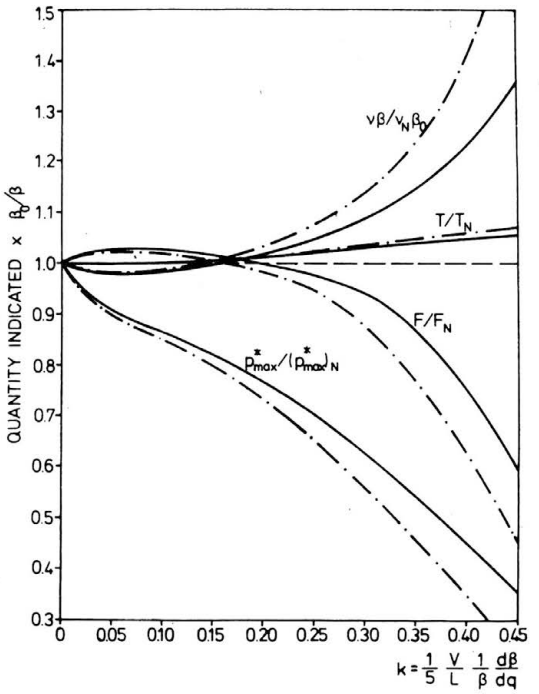

FIG. 4.

In a similar way, the integration of shear stress

(4.4)
$$T=\int_{-\lambda}^{\infty} T^{*12}(\xi)|_{y=\pm h}\,d\xi,$$

after substituting from Eqs. (2.10) and (3.10), gives the total friction force in the form

(4.5)
$$|T|=\frac{3\beta V}{2}\sqrt{\frac{2R}{h_0}}\left\{(1-\lambda^2)\left(\operatorname{atrcg}\lambda+\frac{\pi}{2}\right)-\lambda\right.$$
$$\left.+\left(\frac{4}{5}k\right)\left[\frac{3}{4}\lambda(1-3\lambda^2)\left(\frac{\lambda}{1+\lambda^2}+\operatorname{arctg}\lambda-\frac{\pi}{2}\right)-\frac{3(1-\lambda^2)}{2(1+\lambda^2)}\right]\right\},$$

where the ratio 4/5 should be replaced by 25/36 in the case (II). The ratio $\beta_0|T|/\beta|T_N|$ plotted versus k in Fig. 4 is a weakly increasing function of $k > 0$, taking values always greater than unity.

As a consequence of the relations described by Eqs. (4.3) and (4.5), we can also calculate the corresponding friction coefficient defined as the ratio:

$$\nu = |T|/F. \tag{4.6}$$

The plot of ν versus $k > 0$, presented graphically in Fig. 4 (indicated as $\beta\nu/\beta_0\nu_N$), is practically independent of the extensional viscosity function $\beta(q)$. For small values of k (up to 0.15) this quantity is a little less than unity, and for higher values of k increases significantly. The fact that the friction coefficient in the case of viscoelastic fluids may be less than that for Newtonian fluids is known from the experimental data for lubricating systems (cf. [8, 9]).

4.2. Effect of extension rate or velocities

It happens very frequently that the extensional viscosity function $\beta(q)$ is an increasing function of the extension rates q. This is the case for solutions of high molecular weight or branched polymers, at least in some range of q (cf. [3, 4, 14]).

By way of illustration, we consider the case in which the dependence of β on q can be modelled by a power-law function, viz.

$$\beta(q) = \beta_0(1+\alpha^n q^n), \qquad \frac{d\beta}{dq} = \beta_0 n\alpha^n q^{n-1}, \tag{4.7}$$

where n denotes a power index. Bearing in mind that, according to Eq. $(3.23)_1$

$$k = \frac{K}{5} = \frac{\lambda}{5}\frac{n\alpha^n q^n}{1+\alpha^n q^n}, \tag{4.8}$$

we obtain, for example,

$$\frac{p^*_{\max}}{(p^*_{\max})_N} = \frac{\lambda}{\lambda - \frac{5}{n}k}\{1+\ \ldots\} \tag{4.9}$$

with an expression in the braces exactly the same as that resulting from Eqs. (4.1) and (3.22). On the other hand, we have

$$V = \frac{L}{\alpha}\sqrt[n]{\frac{\lambda^2 k}{10\lambda - k}}, \tag{4.10}$$

since in the case considered: $q = V/L\lambda$.

The plots of the ratio $p^*_{\max}/(p^*_{\max})_N$ versus $k > 0$ and $\alpha V/L$ (for $n = 2$) for several values of n are shown in Fig. 5. It is noteworthy that for higher n ($n = 4$), the ratio considered may be even less than unity in some range of k or V.

In a similar way the plots of the ratios F/F_N and T/T_N can be constructed; the corresponding graphs are omitted.

As we mentioned before, overall dependences of $p^*_{\max}/(p^*_{\max})_N$, F/F_N and T/T_N on the extension rates q or the velocity of rollers V may be different for different ratios $\beta(q)/\beta_0$. By way of further illustration, we consider the case in which the extensional viscosity function is of the form shown schematically in Fig. 6. Such a form corresponds to fluids containing either long branched molecules or long rod-like particles highly orientating in some range of extension rates (or velocity of rollers). Then the coefficient of viscoelas-

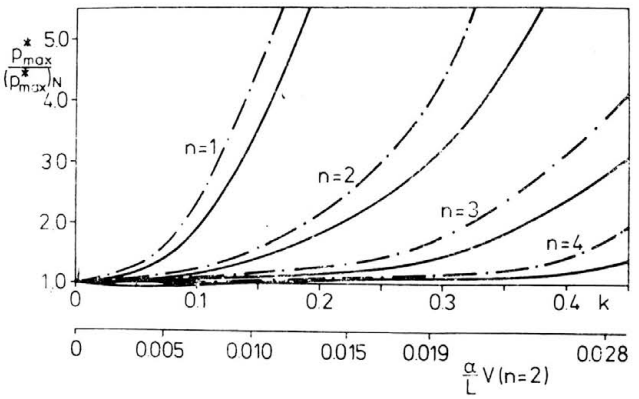

FIG. 5.

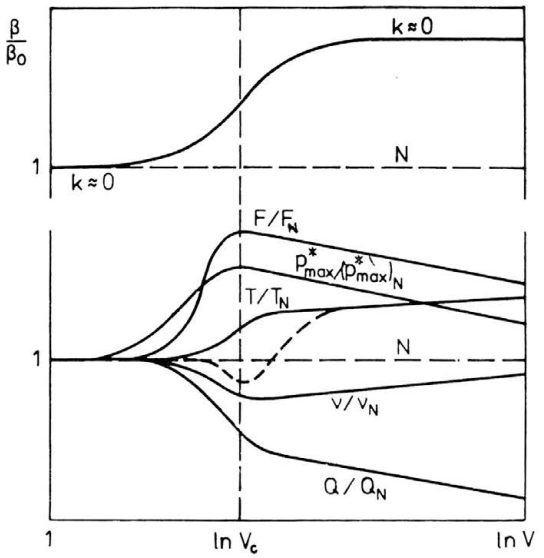

FIG. 6.

ticity k is very small for low velocities, next increases significantly, and finally tends to zero again. The maximum value of $k > 0$ refers to some characteristics extension rate q_c or velocity V_c.

Bearing in mind the results presented in Fig. 4 as well as the above assumed variability of the coefficient k, we can construct qualitative plots of $p^*_{max}/(p^*_{max})_N$, F/F_N, T/T_N, v/v_N and Q/Q_N as functions of ln V. This is shown schematically in Fig. 6 where different scales for ordinates are used.

It is seen that the maximum thrust as well as the total load force may exhibit some maxima corresponding to the characteristic velocity V_c. The total friction force is rather an increasing function of velocity, while the friction coefficient is usually a decreasing function of velocity and may have a minimum. Also the volumetric rate per unit length

of a cylinder is less for viscoelastic fluids than that for Newtonian fluids. The above statements are in qualitative agreement with the experimental measurements and numerical results obtained by P. DOREMUS and J. M. PIAU [8, 9] for aqueous Polyox solutions in a cylinder-plane lubricated contact. The only exception is concerned with the total friction force behaviour since in the paper [8] a minimum of that force was observed (the broken line in Fig. 6) at the velocity of order 0.1 m/s. This important discrepancy can easily be explained, bearing in mind the fact that in our approach based on the notion of flows with dominating extensions (FDE), the shear stresses on the rotating surfaces increase with higher extension rates. For numerous polymeric fluids the so-called shear-thinning phenomenon may be prevailing close to the walls where shearing effects are dominating over extensions, at least in a narrow range of rates.

4.3. Remarks on the rolling bank region

In many rolling or calendering processes, the medium does not enter the nip in a straight -forward way, but the so-called rolling bank region is formed at some distance from the nip. Characteristic features of the rolling bank mechanism are the existence of at least two stagnation points, the lack of symmetry with respect to the plane at half-distance between rollers, and the apparently three-dimensional character of flow. Because of these reasons, the whole problem becomes very complex even for purely viscous fluids (cf. [4]).

Although the solutions presented are valid exclusively in the nip region, some information on the rolling bank flow can be estimated from the present results (cf. [4]). This is possible since even in the Newtonian case different terms in the expression for velocity are of different orders of magnitude. For instance, Eq. (3.15) implies that for $\xi \to \infty$

$$u^* = \frac{\partial \Psi}{\partial y} \to \frac{1}{2} V\left(1-3\frac{y^2}{h^2}\right), \tag{4.11}$$

and

$$\Psi = \int u^* dy \to \frac{1}{2} Vy\left(1-\frac{y^2}{h^2}\right), \tag{4.12}$$

where Ψ denotes the stream function. This function is zero for $y = -h$, 0 and h, and takes a maximum value for $y = h/\sqrt{3}$. Thus the actual flow through the nip is negligible as compared with the limit flow described by Eqs. (4.11) and (4.12). Although the reversed streamlines prevail between 0 and h, there still exists some flow close to the surface of the rollers.

Extending the above reasoning to the case of viscoelastic fluids, we shall apply a slightly different approach than above. First, equating Eq. (3.26) to zero, we obtain

$$\cos\sqrt{\gamma\frac{y^2}{h^2}} = \exp\left(\frac{K}{\xi-\lambda}\right)\cos\sqrt{\gamma}\,; \tag{4.13}$$

what, after expanding the cosine terms into a series, leads to

$$\frac{y^2}{h^2} = 1-\frac{2}{H}\frac{1+\xi^2}{\xi^2-\lambda^2}. \tag{4.14}$$

Taking into account Eqs. (3.39) and retaining terms linear with respect to $k = K/5$, we arrive at

$$\frac{y^2}{h^2} = \frac{1}{3} - \frac{8}{5} k \frac{1}{\xi - \lambda} \tag{4.15}$$

and at a similar expression with 25/18 instead of 8/5 for the case (II). If $\xi \to \infty$, we see that again $y \to \pm h/\sqrt{3}$, but for finite large ξ, the value of y for $k > 0$ will be less and the range of reversed flow diminished. Thus we may conclude that an increasing extensional viscosity function supresses the rolling bank mechanism at some distance from the nip.

It was previously shown that in viscoelastic fluids λ as well as ξ_s decrease for increasing $k > 0$, i.e. the position of maximum thrust as well as the stagnation point approach the nip cross-section. Under more severe conditions, it many happen that the rolling bank region is situated very close to the nip. Equation (4.15) for $\xi \to 0$ leads to

$$\frac{y^2}{h^2} = \frac{1}{3} + \frac{8}{5} \frac{k}{\lambda}. \tag{4.16}$$

Then the value of y may be greater than $H/\sqrt{3}$, leading to a complete stop of flow through the nip, i.e. to the case of fully reversed flow.

5. Conclusions

The concept of plane flows with dominating extensions (FDE) applied to the case of nip flow between two rotating cylinders enables the formulation of the following conclusions:

1) Since in the flow considered the extension gradients are really dominating, at least in the middle part of the nip region, the procedure developed in the paper can be used successfully for viscoelastic fluids, leading to relatively simple analytical and approximate solutions.

2) In particular, the well-known solutions valid for purely viscous Newtonian fluids are rediscovered in a straight-forward way.

3) All the results obtained in the case of viscoelastic fluids essentially depend on the extensional viscosity function and its variability with increasing extension rates. The latter property can be characterized by the viscoelasticity coefficient, defined as the ratio of the extensional viscosity derivative with respect to the extension gradient to the extensional viscosity itself.

4) It was shown that viscoelastic properties of a fluid, in the case of increasing extensional viscosity, reduce significantly the distances from the nip to the exit (the place at which the fluid leaves the rollers) and to the place where the thrust distribution reaches its maximum. Also the stagnation point situated on the entry side of rollers moves closer to the nip. In the case of decreasing extensional viscosity, the above effects are opposite.

5) For small variability of the extensional viscosity function, such quantities as the maximum thrust, the total load force, the total friction force and the friction coefficient can be expressed by products of the two factors: the first factor proportional to increasing or decreasing extensional viscosity, and the second one depending on the viscoelasticity coefficient and the boundary conditions applied.

6) In the case of frequently occurring S-shaped variability of the extensional viscosity function, the maximum thrust and the total load force increase with increasing velocity of rollers, showing the maxima for some characteristic velocity. The total friction force also increases monotonically with increasing velocity of rollers, on the contrary to some experimental observations in which a local reduction of that force was noted. The volumetric rate of flow and the friction coefficient usually decrease for higher velocities; the latter quantity may have a minimum value. In general, the above qualitative picture of the flow considered remains in good agreement with experimental data.

7) Although the solutions presented are valid only in the nip region, some information can be obtained on the so-called rolling bank flow. It seems that the increasing extensional viscosity of a fluid suppresses the reversed flows far from the rollers, but enhances them close to the nip.

References

1. R. E. GASKELL, *The calendering of plastic materials*, J. Appl. Mech., **17**, 334, 1950.
2. A. CAMERON, *Basis lubrication theory*, Ellis Horwood, Chichester 1976.
3. R. S. LENK, *Polymer rheology*, Appl. Sci. Publ., London 1978, Chapter 11.
4. J. R. A. PEARSON, *Mechanics of polymer processings*, Elsevier Appl. Sci. Publ., London-New York 1985, Chapter 13.
5. A. B. METZNER and A. P. METZNER, *Stress levels in rapid extensional flows of polymeric liquids*, Rheol. Acta, **9**, 174, 1970.
6. J. M. BROADBENT, D. C. POUNTNEY and K. WALTERS, *Experimental and theoretical aspects of the two-roll mill problem*, J. Non-Newtonian Fluid Mech., **3**, 359, 1978.
7. J. M. BROADBENT, *Elastic liquid experiments with the four-roll mill and two-roll mill*, Proc. VII Inter. Congress on Rheology, Gothenburg 1980.
8. P. DOREMUS, Thèse de docteur-ingenieur a l'USMG et l'INP de Grenoble, Juin 1982.
9. P. DOREMUS and J. M. PIAU, *Experimental study of viscoelastic effects in a cylinder-plane lubricated contact*, J. Non-Newtonian Fluid Mech., **13**, 79, 1983.
10. R. CRESSLY, R. HOCQUART, O. SCRIVENER, *Biréfringence d'écoulement localisée dans un dispositif à deux rouleaux*, Optica Acta, **25**, 559, 1978.
11. S. ZAHORSKI, *Viscoelastic flows with dominating extensions: application to squeezing flows*, Arch. Mech., **38**, 191, 1986.
12. A. B. METZNER, *Extensional primary field approximations for viscoelastic media*, Rheol. Acta, **10**, 434, 1971.
13. D. R. OLIVER, *The influence of fluid inertia, viscosity and extra stress on the load bearing capacity of a squeeze film of oil*, Appl. Sci. Res., **35**, 217, 1979.
14. S. ZAHORSKI, *Mechanics of viscoelastic fluids*, M. Nijhoff Publ., The Hangue—Boston—London 1982, Chapter 1 and 2.
15. C. M. TAYLOR, *Separation cavitation in highly loaded fluid film bearings with both surfaces in motions*, J. Mech. Eng. Sci., **16**, 147, 1974.
16. I. S. GRADSTEYN and J. W. RYZHIK, *Tables of integrals, series and products*, Academic Press, New York 1965.

POLISH ACADEMY OF SCIENCES
INSTITUTE OF FUNDAMENTAL TECHNOLOGICAL RESEARCH.

Received March 19, 1986.